Large-Scale Circulations Forced by Localized Mixing over a Sloping Bottom[*]

MICHAEL A. SPALL

Department of Physical Oceanography, Woods Hole Oceanographic Institution, Woods Hole, Massachusetts

ABSTRACT

A simple, nonlinear, two-layer, planetary geostrophic model of the large-scale circulation forced by localized mixing over a sloping bottom is discussed. The model is forced by parameterized diapycnal mixing at the density interface and/or by a mass flux downward into (unresolved) deep topographic canyons. Two nondimensional parameters are identified: the ratio of the change in Coriolis parameter over the horizontal mixing length scale to the nominal Coriolis parameter and the ratio of the advective speed to the Rossby wave phase speed. The former controls the strength of horizontal recirculation gyres that are forced by spatially variable diapycnal mixing, while the latter is a measure of the importance of nonlinearity in the density equation. When bottom topography is introduced, bottom pressure torque becomes important and the traditional strong horizontal recirculation gyre found for mixing over a flat bottom (beta plume) is gradually replaced by a zonal flow into or out of the mixing region in the deep ocean. Bottom topography becomes important, and the zonal flow emerges when the topographic Rossby wave speed exceeds the baroclinic planetary Rossby wave speed. Nonlinear effects are shown to enhance the upper-layer recirculation for upwelling and to retard the upper-layer circulation for downwelling. The model is finally configured to represent a region of mixing over the western flank of the Mid-Atlantic Ridge in the deep Brazil Basin. The model upper-layer flow is toward the southwest and the deep flow is very weak, zonal, and toward the east, in reasonable agreement with recent observational and inverse model estimates. The bottom pressure torque is shown to be crucial for maintaining this weak, zonal deep flow in the presence of strong turbulent mixing.

1. Introduction

Recent tracer release and microstructure measurements suggest that diapycnal mixing is greatly enhanced in the vicinity of rough, sloping bottom topography (Ledwell et al. 2000; Polzin et al. 1997). The present study is partially motivated by these observations and the intriguing finding that the deep velocity field is very weak despite the presence of strong turbulent mixing (St. Laurent et al. 2001). These mixing regions are of fundamental importance to the global thermohaline circulation and to budgets of mass, heat, and other tracers. Understanding the circulation forced by such spatially variable mixing patterns is necessary to further our understanding of the abyssal circulation and the upwelling component of the general thermohaline circulation.

The traditional view of the buoyancy-forced abyssal circulation is based on the seminal work of Stommel and Arons (1960). They recognized that a weak poleward flow would be required to balance the large-scale

downward diffusion of heat into the abyss and, through continuity, inferred that strong deep western boundary currents must exist to provide mass for the interior upwelling regions. They represented the abyssal ocean as a single moving layer and specified the vertical velocity as a function of space. Weak bottom topography is allowed by the theory, provided that the potential vorticity contours intersect the eastern boundary of the domain. Key aspects of this theory are that in the deep ocean linear vorticity dynamics hold, buoyancy forcing is dominant, and the downward diffusion of heat is balanced locally by upwelling.

Several investigators have extended this type of model to consider the circulations forced by large-scale upwelling when topography is sufficiently strong to introduce regions of closed potential vorticity contours. Straub and Rhines (1990) showed that a seamount or depression modifies the traditional Stommel–Arons circulation by introducing a strong recirculation over the topography and two zonal jets that connect the region of strong topography to the western boundary. Similar results were found by Kawase and Straub (1991) in a single layer shallow-water model with a mass source. Kawase (1993) extended this source-driven shallow water model to consider topographic variations on the basin scale. It was found that, for a basin that does not cross the equator, the weak poleward flow of Stommel and

Corresponding author address: Dr. Michael A. Spall, Woods Hole Oceanographic Institution, MS21, Woods Hole, MA 02543.
E-mail: mspall@whoi.edu

Arons is replaced by a basinwide cyclonic circulation with no western intensification. Basins with topography that cross the equator show circulation patterns very similar to that found for a flat bottom. Straub et al. (1993) also considered strong topography on the basin scale subject to both large-scale and localized forcing. They emphasize the importance of topography and non-linearities in controlling the characteristic pathways and introducing boundary layers in regions where characteristics converge.

The baroclinic nature of the abyss is far more complex than can be represented accurately in a depth-averaged model such as used by Stommel and Arons. Joyce and Speer (1987) derived a linear, flat-bottomed, continuously stratified counterpart of the Stommel–Arons abyssal circulation model in which they could imbed localized temperature anomalies. They showed that the nature of the circulation and tracer distribution depends strongly on the ratio of the advective speed to the Rossby wave phase speed. Circulation anomalies, relative to the barotropic Stommel–Arons circulation, can extend eastward or westward depending on the depth in the water column and the strength of the thermal forcing. In the limit of very large Rossby wave phase speeds, the temperature anomaly is connected to the western boundary through two recirculating zonal jets connected by a strong meridional flow in the region of mixing. In this limit, their results are analogous to the beta plumes introduced by Stommel (1982). Pedlosky (1992) showed that zonal variations in the upwelling rate out of a stratified abyss would force a strongly baroclinic circulation with reversals in the meridional velocity with depth.

Most simple abyssal circulation models make the implicit assumption that the density equation is linear and obeys a local, one-dimensional balance between vertical advection and vertical diffusion. This allows one to infer the vertical velocity from estimates of the vertical diffusivity and stratification. Once the vertical velocity is determined, the horizontal circulation can be calculated by assuming a linear vorticity balance and the appropriate boundary conditions. Such a linearization of the density equation is a good approximation in the limit that the isopycnal slope is small. However, as the isopycnal slope becomes steep, the horizontal velocity component across the sloping isopycnal can contribute significantly to the diapycnal advection. The general parametric dependence of these nonlinear terms in the density equation, when they might be expected to be large, and their potential role in the general circulation remains unclear.

Hautala and Riser (1989, hereafter HR) developed a three-layer model of the wind- and buoyancy-driven circulation, including bottom topography, that takes into account some of these nonlinear terms in the density equation. Their model was forced with a specified wind stress curl and cross-isopycnal mass flux (intended to represent turbulent mixing processes or geothermal sources). However, the model retains the nonlinear den-
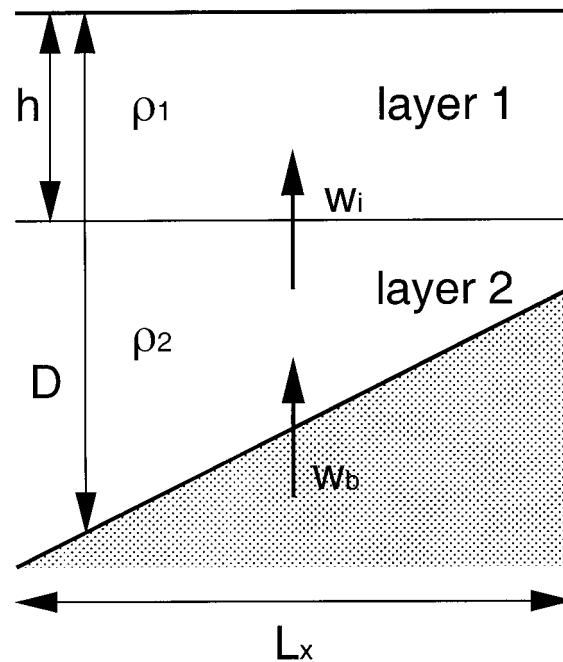

FIG. 1. Schematic of the model configuration. The upper layer has thickness h; the depth of the fluid is D. The fluid is stably stratified with $\rho_2 > \rho_1$. Turbulent mixing at the fluid interface is parameterized as a diapycnal mass flux w_i, and mass flux into deep (unresolved) canyons is represented by w_b.

sity equation terms only in the main thermocline and neglects the nonlinear interaction between the abyssal circulation and the middepth ocean. This confines the topographic influences to the deepest layer. They applied their model to basin-scale circulations with midocean ridges and subtropical gyre wind forcing.

The present study considers the large-scale circulation forced by localized, spatially variable mixing over a sloping bottom. This study differs from previous works by focusing on the influences of nonlinearities in the density equation on the abyssal and upper-ocean flow and potential vorticity field, the circulation and mass budget required to balance *localized* mixing regions over a sloping bottom, and the dependence of the deep and intermediate circulations on a mixing rate that increases toward a sloping bottom.

The nondimensional form of the nonlinear, two-layer characteristic equations are derived and interpreted in terms of wave dynamics, geostrophic velocities, and bottom pressure torque in section 2. In section 3, analytic linear and nonlinear solutions, as well as numerical integrations of the characteristic equations, are applied to several idealized examples to illustrate the influences of a sloping bottom and nonlinearities on the large-scale circulation and potential vorticity distribution forced by localized diapycnal mixing. Finally, in section 4, the model is configured to represent the region of strong diapycnal mixing over the western flank of the Mid-
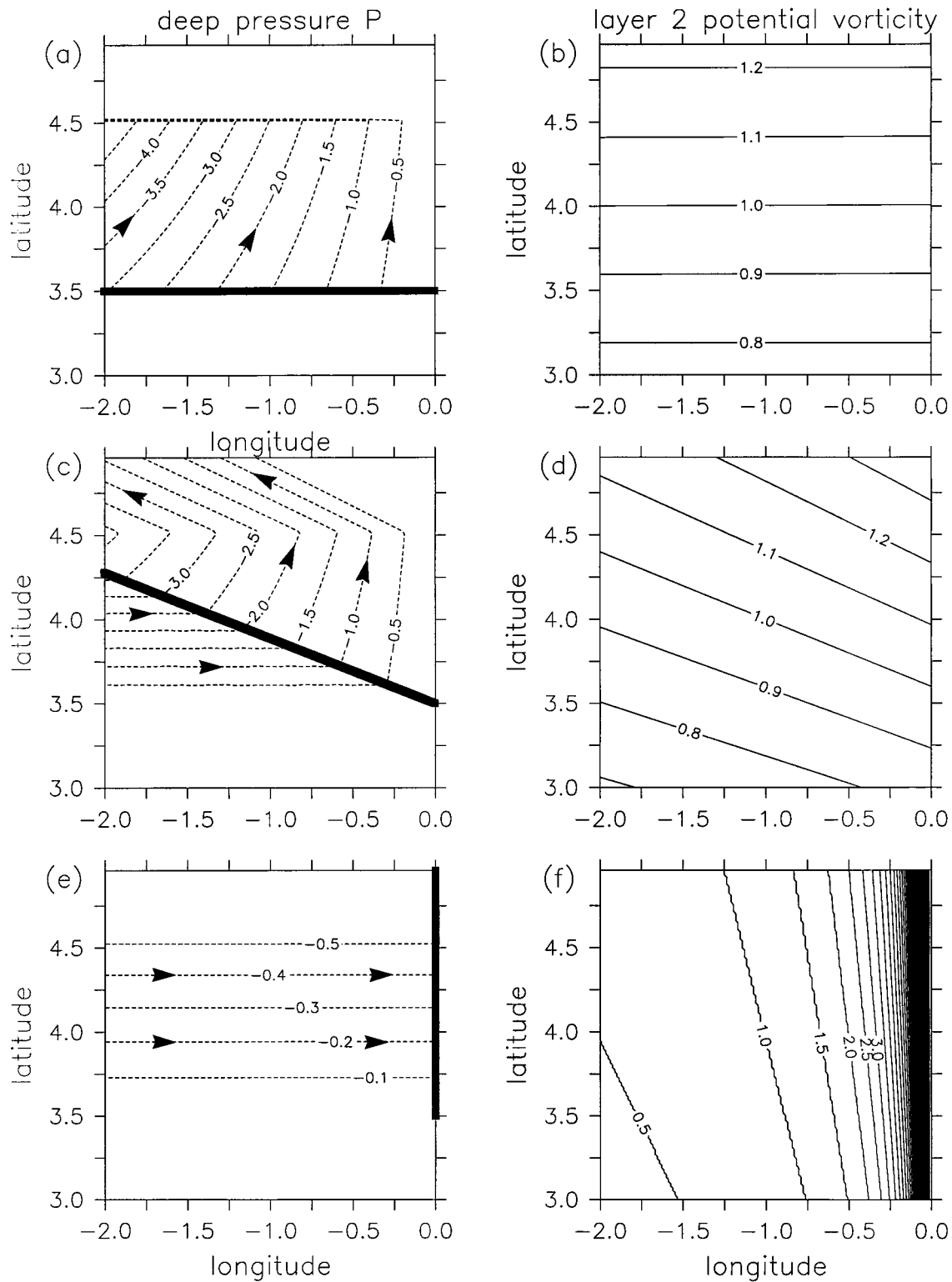
FIG. 2. The deep pressure (and flow direction) and potential vorticity for flat bottom (a) and (b), weak bottom slope $D_x = -0.1$ (c) and (d), and strong bottom slope $D_x = -1.0$ (e) and (f). The bold line on the pressure fields marks the critical characteristic that originates from the southeastern corner of the mixing region and separates the western, topographically dominated regime from the eastern, turbulent-mixing-dominated regime.
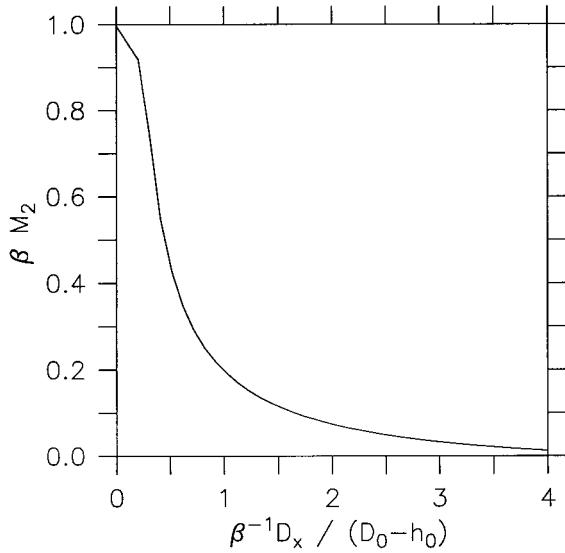
FIG. 3. Strength of the deep meridional flow at $y = y_0$, scaled by β^{-1}, as a function of the deep characteristic slope, which is also the ratio of the topographic Rossby wave phase speed to the baroclinic Rossby wave phase speed.

Atlantic Ridge in the Brazil Basin. The main points are summarized in section 5.

2. Dynamics and the characteristic equations

The nondimensional equations of motion governing the large-scale circulation forced by diapycnal mixing between two fluid layers of different density over a sloping bottom are derived. It is assumed that the large-scale circulation is governed by planetary geostrophic dynamics. The horizontal flow is geostrophic, but the horizontal divergences arising from the spatial variation in the Coriolis parameter, diapycnal mass fluxes, and the presence of bottom topography are retained. The equations also allow for large spatial variations in the stratification, or thickness of the isopycnal layers, and bottom depth. The diapycnal mixing due to small-scale turbulence is represented as a mass flux across the density interface.

A schematic of the model configuration is shown in Fig. 1. There are two moving layers in a finite depth ocean and the bottom pressure torque term (e.g., see Holland 1973 or Mertz and Wright 1992) is included. The thickness of the upper layer is h, the depth of the fluid is given by D, and the dynamic pressure in layer 2 is P. The stratification is represented by the reduced gravity between the two layers, given by $g' = g(\rho_2 - \rho_1)/\rho_0$, where ρ_0 is a reference density for seawater. The diapycnal mixing is represented as a specified mass flux w_i across the density interface. For simplicity, the bottom slope is assumed to vary in the zonal direction only with uniform slope D_x as $D = D_0 + D_x(x + L_x/2)$, where L_x is the zonal extent of the domain, D_0 is the depth at $x = -L_x/2$, and $x = 0$ on the eastern boundary.

A mass flux through the bottom, w_b, is also permitted. This lower boundary condition is motivated by recent mass budgets based on tracer release and microstructure measurements in the deep Brazil Basin, where it has been found that there is a significant net downward mass flux from the interior of the deep basin into narrow canyons in the sloping bottom (Ledwell et al. 2000; St. Laurent et al. 2001). This downward mass flux is required to balance a turbulent diffusion that increases strongly toward the bottom. Once in the canyons, the mass is believed to be fluxed across sloping density surfaces toward lighter density through turbulent mixing. The deep flow in the channels is not explicitly represented here, but the mass flux into the deep channels is accounted for and returned to the upper layer where the density interface intersects the bottom. In this configuration, the deep layer in the model is intended to represent the deep flow above the depth of strong diapycnal upwelling in the canyons.

The characteristic equations are derived by substituting the geostrophic relations into continuity equations to obtain vorticity equations for the two moving layers. These two equations may be manipulated to form a characteristic equation for the deep pressure P and a diagnostic equation that relates the interface depth h to P and the forcing. The dimensional form of the equations, and scaling for nondimensionalization, are derived in the appendix. The nondimensional form of the equations are solved and discussed in the remainder of this paper. The characteristic equation for the pressure in the deep layer is written in terms of the characteristic velocities as

$$\frac{dx}{ds}P_x + \frac{dy}{ds}P_y = \frac{dP}{ds}, \qquad (1)$$

where s is the direction along the characteristics. The nondimensional characteristic velocities are defined as

$$\frac{dx}{ds} = \left[\frac{h(D - h)}{y} - \epsilon(S_1 + W_B + \beta S_3)_y\right] \quad \text{and} \quad (2)$$

$$\frac{dy}{ds} = -\left[1 + \epsilon\frac{\beta y P_y}{h} + \epsilon\frac{(\beta y)^2 w_b}{h D_x}\right]h D_x. \qquad (3)$$

The change in pressure along the characteristic is given by

$$\frac{dP}{ds} = \beta y h(w_b - w_i). \qquad (4)$$

There are two important nondimensional numbers, $\beta = \beta^* L/f_0$ and $\epsilon = U/\beta^* L_d^2$, where $L_d = (g'H)^{1/2}/f_0$ is the internal deformation radius and β^* is the meridional gradient of the Coriolis parameter. The variation of the Coriolis parameter over the spatial scale of mixing L, relative to the nominal value of the Coriolis parameter f_0, is given by β. This parameter was shown by Spall (2000) to control the strength of the horizontal recir-
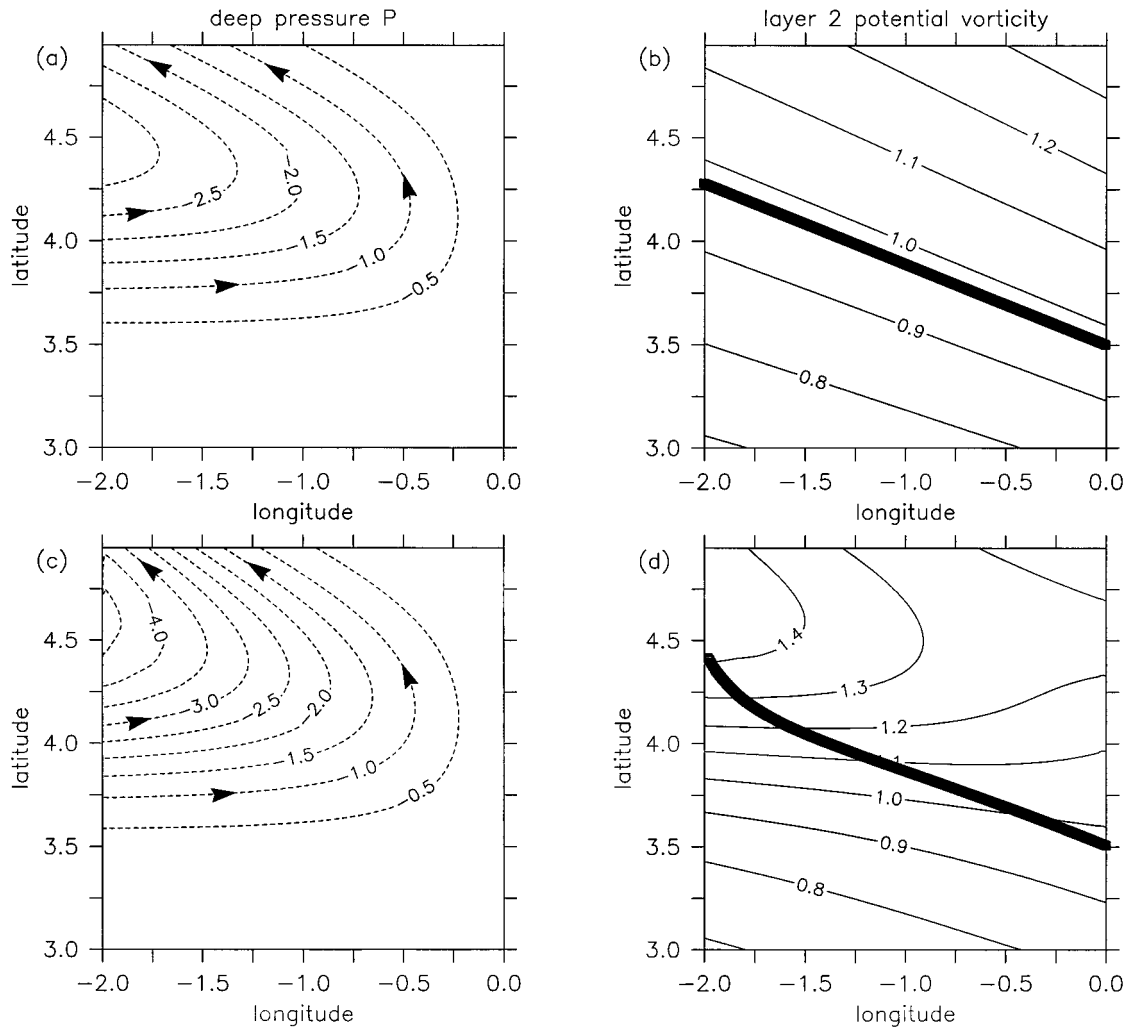
FIG. 4. Deep fields for weak bottom slope ($D_x = -0.1$) with exponentially decaying upwelling of strength $w_0 = 0.5$ in the linear limit ($\epsilon = 0.001$) pressure (a), potential vorticity (b) and for moderate nonlinearity ($\epsilon = 0.25$) pressure (c) and potential vorticity (d). The bold line on the potential vorticity fields marks the critical characteristic that originates from the southeastern corner of the mixing region and separates the western, topographically dominated regime from the eastern, turbulent-mixing-dominated regime.

culation gyre forced by diapycnal mixing over a flat bottom. The terms S_1 and S_3 arise as a result of nonlinear interactions between the deep flow and the bottom topography, while W_B is due to a vertical mass flux into the bottom. These terms are defined in (8) and described in physical terms in the appendix.

The parameter ϵ is the ratio of the advective velocity U to the baroclinic Rossby wave phase speed. For weak advection, or strong stratification, the interface displacement is small compared to the resting layer thickness. As the stratification is reduced, ϵ increases and the interface displacement required to balance the thermal wind increases.

The slope of the characteristics is given by

$$\frac{dy}{dx} = \frac{(1 + \epsilon\beta y P_y/h + \epsilon(\beta y)^2 w_b/hD_x)yD_x}{(D - h) - \epsilon y(S_1 + W_B + \beta S_3)_y}. \quad (5)$$

In the linear limit ($\epsilon = 0$) advective effects are negligible and the characteristic slope is simply the slope of contours of uniform potential vorticity in the deep layer. The nondimensional potential vorticity of layer 2 is given by $q_2 = \beta y/(D - h)$ and the slope of the potential vorticity contours is

$$\frac{dy}{dx} = -\frac{dq_2}{dx}\frac{dy}{dq_2} = \frac{yD_x}{(D - h)}. \quad (6)$$

In the limit of weak nonlinearity the interface is essentially flat ($h = h_0$) and advection is weak. The characteristic paths are controlled by the competition between the planetary vorticity gradient and the thickness of the deep layer. This characteristic slope is also the ratio of the topographic β to the planetary β, or the topographic Rossby wave phase speed to the planetary Rossby wave speed. For topography that slopes upward

to the east, the topographic Rossby wave phase speed is poleward and the zonal phase speed is to the west so that $dy/dx < 0$ and the characteristics enter the mixing region from the eastern and the equatorward side.

When $\epsilon \neq 0$, the characteristics within the forcing region over the sloping bottom are no longer lines of constant potential vorticity, although they do coincide with potential vorticity contours outside the region of active mixing and over a flat bottom. As nonlinearity increases, and advection becomes important, the characteristics speed up or slow down as a result of the barotropic geostrophic velocities generated by the bottom pressure torque and mass flux into the bottom. This barotropic flow forces the characteristics to cross potential vorticity contours. This is equivalent to the competition between the planetary Rossby wave phase speed and the wind-driven Sverdrup flow discussed by Luyten and Stommel (1986), although they did not relate it to the nonlinearity of the density equation. As will be shown in section 3, regions of isolated potential vorticity contours can be generated and forced into motion by the diapycnal mixing over a sloping bottom. However, if nonlinearities are sufficiently strong, the advective velocities can overwhelm the phase speed of the waves and reverse the direction of the characteristics. This coincides with the development of a region that is blocked from characteristic access from the equatorward side and the east, a situation that is not considered here.

The barotropic vorticity equation is used to relate the thickness of layer 1 to the properties of the deep layer:

$$h^2 = h_0^2 - 2\epsilon(S_1 + \beta S_2 + W_B). \quad (7)$$

The terms S_1, S_2, S_3, W_B retain the same physical interpretations as discussed for the dimensional equations in the appendix, but are calculated from the nondimensional variables as follows:

$$S_1 = \int_0^x \beta y D_x P_y \, dx, \qquad S_2 = \int_0^x DP_x \, dx,$$

$$S_3 = \int_0^x D_x P \, dx, \qquad W_B = \int_0^x (\beta y)^2 w_b \, dx. \quad (8)$$

The geostrophic relations are written in nondimensional form as

$$u_2 = -\frac{P_y}{\beta y}, \qquad v_2 = \frac{P_x}{\beta y}, \quad (9)$$

$$u_1 = -\frac{(P + \epsilon^{-1}\beta^{-1}h)_y}{\beta y}, \qquad v_1 = \frac{(P + \epsilon^{-1}\beta^{-1}h)_x}{\beta y}. \quad (10)$$

The deep flow is along lines of constant P although, because the flow is horizontally divergent, the pressure is not the same as a streamfunction. The upper-layer flow is along lines of constant $P + \epsilon^{-1}\beta^{-1}h$, but once again the flow is horizontally divergent along this path.

The solution procedure is as follows. The pressure in layer 2 and the interface height h are specified along the eastern and southern boundaries of the mixing region. The strength of the diapycnal mixing is specified as a function of space through w_i and the strength of the mass flux into the narrow canyons in the sloping bottom is specified through w_b. It is assumed here that the turbulent mixing rates w_i and w_b are independent of the large-scale mean abyssal circulation, as would be expected if they are driven primarily by tidal interaction with the bottom topography. The pressure in the deep layer is calculated by integrating along the characteristic paths as they transverse the model domain. On the first iteration, the nonlinear terms are assumed to be zero and linear solutions for P and h are obtained. The terms S_1, S_2, S_3, and W_B are then calculated from the first guess for P and h. The modified solutions for P and h are obtained with these updated forcing terms. This iterative procedure is followed until the solution has converged, usually after only a few (less than ten) iterations. The results presented below have been obtained by integrating along 300 characteristics initially uniformly distributed along the eastern and equatorward boundaries. The data are then interpolated back onto a uniform 150×150 grid for plotting and diagnostics.

While this approach is clearly very idealized, it allows for approximate linear and weakly nonlinear closed form solutions to be obtained, which include the bottom pressure torque terms, and provides complete nonlinear solutions through numerical integration. The idealized approach also identifies and lends simple interpretation to the critical characteristic pathways and nondimensional parameters that control the structure of the deep circulation and the relative magnitude of the nonlinear terms.

3. Large-scale circulation examples

a. Topographic effects: Linear regime

The effects of a sloping bottom are most clearly demonstrated by considering the large-scale circulation forced by a localized region of diapycnal mixing when nonlinearities are small. Consider first the case of a localized region of uniform mixing over a flat bottom. An example is carried out for which $w_i = 0.5$ between $3.5 < y < 4.5$, outside of this region $w_i = 0$. The zonal extent of the basin is $-2 < x < 0$. The upper-layer thickness $h_0 = 4$ and the depth $D_0 = 5$, appropriate for diapycnal mixing of an abyssal water mass. The basic dynamics are most easily revealed by setting the mass flux into the lower boundary to zero, $w_b = 0$. Because the main interest here is to understand the circulation forced by such a local region of diapycnal mixing, the deep pressure is set to zero along the eastern and southern boundaries. Influences from distant regions could be included by specifying $P = P(x)$ at the southern limit of mixing. The Coriolis parameter is appropriate for a midlatitude mixing region, $\beta = 0.25$, and nonlinearities are small, $\epsilon = 0.001$.

1) FLAT BOTTOM

The deep pressure P resulting from this localized mixing over a flat bottom is shown in Fig. 2a. There exists a broad meridional flow with narrow jets extending to the west at the northern and southern limits of mixing. In this case, the potential vorticity is controlled by the planetary vorticity gradient and the characteristics are purely zonal (Fig. 2b). This is the beta-plume circulation discussed by Stommel (1982), Joyce and Speer (1987), Pedlosky (1996), and Spall (2000). The strength of the horizontal recirculation gyre compared to the total amount of upwelled water is $O(\beta^{-1})$. This can be calculated directly from the characteristic equations by first calculating the zonal pressure gradient at $y = y_0$ as

$$P_x = \frac{dP}{ds}\frac{ds}{dx} = \frac{\beta y^2 w_i}{D - h}. \tag{11}$$

The meridional transport in layer 2, M_2, is calculated by zonally integrating across the region of diapycnal mixing from $x = -L_x$ to $x = 0$, with $y = y_0 = \beta^{-1}$, to give

$$M_2 = \int_{-L_x}^{0} \frac{P_x(D - h)}{\beta y} \, dx = \beta^{-1}L_x w_i. \tag{12}$$

For the present example, $w_i L_x = 1$ and $M_2 = \beta^{-1} = 4.0$ at the midlatitude of the mixing region.

The transport in the upper layer is of the same strength but in the opposite direction (anticyclonic). The depth-integrated transport over a flat bottom vanishes for $\epsilon \ll 1$. This strong horizontal recirculation is required in order to balance the vertical velocity w_i. The change in pressure from the eastern boundary to the western boundary, and hence the meridional transport, increases with increasing latitude because the Rossby wave phase speed decreases with latitude. This gives rise to a meridional pressure gradient at $x = -L_x$ and a zonal (eastward) flow into the mixing region required to balance mass.

2) WEAK BOTTOM SLOPE

The introduction of even a weak bottom slope changes the deep flow significantly. The deep pressure for a case with $D_x = -0.1$ is shown in Fig. 2c. This bottom slope is equivalent to a change in the depth by 10% of H over a horizontal distance L. The potential vorticity contours now slope toward the north and west because of the change in the lower-layer thickness (Fig. 2d). The narrow jet at the southern limit of mixing that supplied the mass for the meridional flow in the flat bottom case has broadened so that there is a uniform zonal flow into the mixing region from the west. This zonal flow turns abruptly to the northeast before flowing out of the mixing region to the north. Once out of the mixing region, the deep flow is along contours of uniform potential vorticity toward the northwest.

The boundary that separates the region of zonal flow from the region of strongly meridional flow is the characteristic trajectory that originates at the intersection of the southern limit of diapycnal mixing and the eastern boundary. This characteristic is indicated on each of the pressure fields in Fig. 2 by the bold line originating at $x = 0$, $y = y_s$. For the case of a flat bottom, this characteristic remains at the southern limit of the mixing region and the flow is primarily meridional (Fig. 2a). However, as topography is introduced, this characteristic veers to the north through the mixing region and opens up a new regime in which the flow is zonal (Fig. 2c).

An analogous zonal flow regime is discussed by Pedlosky (1987) for a barotropic quasigeostrophic wind-driven flow over a sloping bottom. The analysis here builds on this simple example to consider planetary geostrophic dynamics (and the attendant mass budget considerations), nonlinearities in the density equation, and a strongly sloping bottom.

Within the region to the west of the critical characteristic, where the flow is zonal, the deep pressure field may be calculated explicitly by integrating along the characteristics. The pressure at latitude y is calculated by integrating along the characteristic from the southern limit of mixing (where $y = y_s$ and $P = 0$) to give

$$P = \int_{y_s}^{y} P_s s_y \, dy = \frac{\beta(y^2 - y_s^2)w_i}{2D_x}. \tag{13}$$

Because w_i and D_x are functions of y only, the pressure anomaly is independent of x, provided that there is no externally imposed pressure gradient to the south of the mixing region. Therefore, the resulting layer 2 geostrophic flow is purely zonal and uniform,

$$u_2 = -\frac{P_y}{\beta y} = -\frac{w_i}{D_x}. \tag{14}$$

For upwelling ($w_i > 0$) and topography that slopes upward to the east, $P_y < 0$, $D_x < 0$, and $u_2 > 0$. The vertical velocity at the bottom is simply $-u_2 D_x = w_i$. The deep flow is zonal because it experiences no stretching in the vertical. The vertical velocity induced by the interaction of the zonal flow with the bottom exactly balances the diapycnal velocity w_i. This stretching at the bottom is due to the bottom pressure torque term discussed by Holland (1973) and Mertz and Wright (1992). Recall that in the linear limit the vertical velocity is due only to diapycnal motions. The mass budget in the deep layer is satisfied by the zonal derivative of the zonal transport:

$$[(D - h)u_2]_x = [(D_0 - h_0 - D_x x)w_i/D_x]_x = -w_i. \tag{15}$$

The upwelling w_i is balanced by a zonal mass flux divergence that is achieved by the uniform zonal flow into a region of uniformly decreasing layer thickness. This regime of zonal flow will be referred to as the western, or topographically dominated, regime.

The flow and mass budget to the east of the critical characteristic are very different from that to the west.

The flow in the east is nearly meridional in the deep layer with a weak zonal component to the east. The pressure in this region may be calculated by integration along the characteristics entering from the eastern boundary to be

$$P = \frac{x\beta y^2 w_i}{D - h}\left(1 - \frac{xD_x}{2(D - h)}\right) + O(\beta^2). \quad (16)$$

This result is very similar to the flat bottom pressure field (11) except for the additional term proportional to the bottom slope D_x. For midlatitudes, $xD_x/2(D - h) = O(\beta) \ll 1$ so that the second term is small compared to the first. Terms of higher order in β have been neglected. The zonal flow is calculated as

$$u_2 = \frac{2xw_i}{D - h}\left(1 - \frac{xD_x}{2(D - h)}\right) + O(\beta^2). \quad (17)$$

The zonal flow vanishes at the eastern boundary ($x = 0$), increases linearly toward the west, and is independent of latitude. Once again, the similarity with the flat bottom beta plume is evident. Bottom pressure torque is very weak here, $O(\beta)$, and the flow is forced primarily by the cross-isopycnal mixing.

The meridional flow is

$$v_2 = \frac{yw_i}{(D - h)}\left(1 - \frac{2xD_x}{(D - h)}\right) + O(\beta^2). \quad (18)$$

The meridional flow is-only a weak function of longitude and increases with latitude. This is the equivalent of the traditional beta plume, rotated and modified slightly by bottom topography. It is clear that the strength of the meridional flow is proportional to the stretching in the deep layer. The stretching is reduced below that forced by the diapycnal velocity w_i by an amount u_2D_x [second term in (18)] due to the interaction of the deep zonal flow with the bottom. Note that, for midlatitudes, this bottom-induced vertical velocity is much smaller than the diapycnal velocity so that v remains $O(y \approx \beta^{-1})$.

The zonal mass flux divergence is $[(D - h)u_2]_x = 2w_i$ while the meridional mass flux divergence is $[(D - h)v_2]_y = w_i$ so that the sum balances the net diapycnal mass flux. The strength and direction of the circulation are analogous to the circulation in the upwelling region of the beta plume over a flat bottom and so will be referred to as the eastern, or beta-plume, regime.

3) STRONG BOTTOM SLOPE

In the limit of very tall topography the entire mixing region is within the topographic regime and the meridional recirculation that characterizes the beta plume is eliminated. An example of the deep pressure field for $D_x = -1.0$, so that the thickness of the deep layer vanishes at the eastern boundary, is shown in Fig. 2e. The corresponding potential vorticity contours are now near-

ly meridional (Fig. 2f) and the critical characteristic is coincident with the eastern boundary. The flow is everywhere zonal and weak; the net transport into the mixing region is just sufficient to balance the net diapycnal mass flux into layer 1 (note the change in contour interval in Fig. 2e). In this limit the deep flow is independent of the boundary condition at $x = 0$ because all of the characteristics originate from the southern boundary. The information is propagated along characteristic trajectories, not the streamlines of the flow that enter from the west.

The strength of the transport in the deep layer depends on the pathways and speed at which the characteristics pass through the mixing region. For a flat bottom, the characteristics are purely zonal and the meridional mass flux is given by (12). As topography is introduced, the characteristics turn toward the north due to the influence of topographic Rossby waves. The integrated influence of the diapycnal mixing on the pressure anomaly, and hence the net transport in the deep layer, depends on how long it takes the characteristics to pass through the mixing region. For very weak bottom slopes, the pressure anomaly is limited by the time it takes the trajectories to exit from the western side of mixing and the recirculation strength is given by (12).

The introduction of significant bottom topography increases the propagation speed of the characteristics through the influence of topographic Rossby waves and the strength of the deep recirculation gyre is reduced. This reduction in meridional transport is large when the slope of the potential vorticity contours in layer 2 (or the ratio of the topographic Rossby wave phase speed to the baroclinic planetary Rossby wave phase speed) is greater than the aspect ratio of the mixing region,

$$\frac{dy}{dx} \approx \frac{\beta^{-1}D_x}{(D_0 - h_0)} > \frac{L_y}{L_x}. \quad (19)$$

The total meridional transport in the deep layer at $y = y_0$ is shown as a function of the linear characteristic slope in Fig. 3. For a flat bottom the strength of the deep recirculation is β^{-1}. This recirculation rapidly decreases with increasing characteristic slope. The previous example for weak bottom topography ($D_x = -0.1$) in Fig. 2b has characteristic slope of $dy/dx \approx -0.4$ and $L_y/L_x = 0.5$. This dependence is essentially the same even when nonlinearities are large, as discussed further below.

This reduction in meridional transport may also be understood in terms of the beta-plume and topographically dominated regimes discussed above. When the topography is flat the entire region is within the beta-plume regime and the meridional flow is forced entirely by w_i. With increasing topography the beta-plume regime diminishes in extent. Since the stretching at the bottom cancels the diapycnal mixing in the topographic regime, the meridional transport is confined to an ever
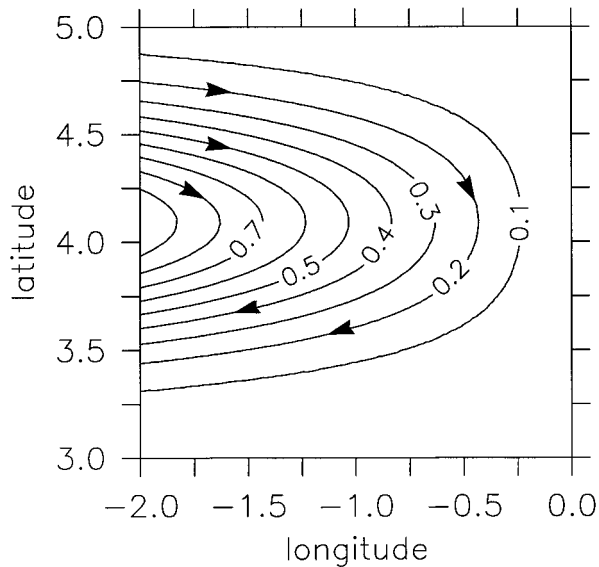
FIG. 5. Streamlines and flow direction for layer 1 ($P + \epsilon^{-1}h^{-1}$) forced by upwelling with an exponential decay and a flat bottom.

smaller fraction of the mixing region and the total meridional transport decreases.

b. Topographic effects: Nonlinear regime

For sufficiently large interface displacements, the horizontal component of the diapycnal velocity (the nonlinear term $\mathbf{v} \cdot \nabla h$) is not neglegible. It is anticipated that such a horizontal component will be important for the large-scale circulation, which is essentially controlled by the linear vorticity balance and the vertical derivative of the vertical velocity. The nonlinear effects here are confined to the density equation; the vorticity equation remains linear.

The influence of the nonlinear terms is demonstrated using a diapycnal mixing distribution $w_i = w_0 e^{-(y/l)^2}$, where $l = 0.5$. This exponential decay in the mixing rate allows for a more extensive exploration of parameter space than can be attained for uniform mixing with an abrupt transition to zero mixing. The zonal jets that result in the uniform mixing case can give rise to very strong vertical velocities at the bottom and cause a reversal of the characteristic velocities even for very small values of ϵ. The exponentially decaying mixing rate retains the essential aspects of the nonlinear terms while avoiding discontinuities in the velocity field.

An example of the deep layer circulation and potential vorticity field with upwelling $w_0 = 0.5$, weak bottom slope ($D_x = -0.1$), $\beta = 0.25$, and $\epsilon = 0.001$ is shown in Fig. 4. The deep flow is dominated by a broad eastward flow into the mixing region, which then turns toward the northwest along potential vorticity contours. This is similar to the circulation found with uniform upwelling (Fig. 2b), but the transitions between regimes

are less abrupt. The critical characteristic is indicated by the bold line and is coincident with a line of constant potential vorticity. The influences of increasing nonlinearity are demonstrated in Figs. 4c,d for a case with $\epsilon = 0.25$. The strength of the deep flow has increased by approximately 30% (consistent with the theory in the following section), although the deep transport has not changed significantly because the thickness of the lower layer has decreased by a corresponding amount.

The deep potential vorticity field is now nearly zonal within the region of mixing as a result of changes in the interface depth and thickness of the deep layer (Fig. 4d). The potential vorticity in the northern part of the domain is increased because the interface slope required to balance the horizontal circulation becomes large with increasing ϵ. The characteristics now cross potential vorticity contours, as demonstrated by the critical characteristic included in Fig. 4d. This crossing is forced by the bottom pressure torque terms, as indicated by (5). For sufficiently strong stretching at the bottom, there will be introduced a region of maximum in potential vorticity contours in the northwest region of mixing (e.g., $q_2 > 1.3$). This region is not isolated from the rest of the abyss, however, as the characteristics are able to penetrate and directly drive the circulation there. This direct driving is different from previous linear and single-layer models with topography in which the circulation within regions of closed potential vorticity contours are controlled by diffusion and eddy fluxes.

The upper-layer circulation for the linear calculation is shown in Fig. 5. The strength of the recirculation at $y = y_0$ is the same as found for the uniform mixing case, but now the very narrow zonal jets that connect the mixing region to the western boundary are replaced by smoothly varying, large-scale flows. The strength of the upper-layer recirculation, in the absence of nonlinear effects, scales as β^{-1}. The general characteristics of the upper-layer flow are insensitive to variations in ϵ and D_x.

The magnitude of the upper-layer recirculation, as measured by the maximum zonal transport into the mixing region, is shown in Fig. 6a as a function of bottom slope and nonlinearity for a case with upwelling of strength $w_0 = 0.5$ and $\beta = 0.25$. There is only weak dependence of the upper-layer recirculation strength on bottom slope when nonlinearities are small ($\mathbf{v} \cdot \nabla h \approx 0$). This is because the vertical velocity is equal to the imposed diapycnal velocity as long as the interface slope is small. This is the limit considered by HR. The strength of the recirculation is also independent of nonlinearity when the bottom is flat. This is because there is no barotropic component and $\mathbf{v} \cdot \nabla h = 0$ for a baroclinic geostrophic flow so, once again, the horizontal advection term vanishes. However, the upper-layer recirculation increases with increasing nonlinearity for weak bottom slopes. This dependence on nonlinearity is reduced, but still present, as the bottom slope increases.
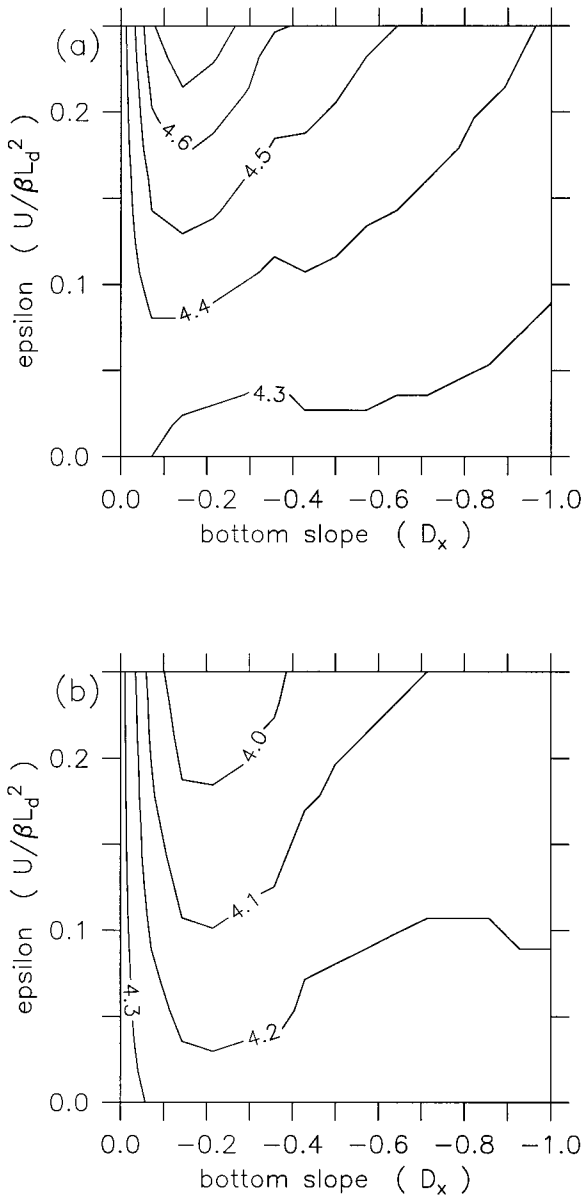
The upper-layer recirculation strength decreases with

FIG. 6. Magnitude of the upper-layer recirculation as a function of nonlinearity $\epsilon = U/\beta*L_d^2$ and bottom slope D_x for (a) upwelling $w_0 = 0.5$ and (b) downwelling $w_0 = -0.5$.

increasing nonlinearity for a downward diapycnal mass flux, as shown in Fig. 6b for $w_0 = -0.5$. The dependence on ϵ is somewhat weaker than it is for the upwelling case; however, the maximum effect is again located at weak, but nonzero, bottom slopes.

In order to understand the sensitivity of the upper-layer circulation to ϵ, the deep circulation and the interface displacement need to be explored in more detail. The linear potential vorticity balance requires that the thickness of layer 1 increase (decrease) toward the west for $w_i > 0$ ($w_i < 0$). This change in h gives rise to a meridional flow required to balance the stretching w_i.

The zonal slope of the interface depth is estimated from (7), for $\epsilon \ll 1$, to be

$$h_x = -\epsilon\beta(yD_xP_y + DP_x) + O(\epsilon^2). \qquad (20)$$

The largest influence of the nonlinear terms arises as a result of the horizontal velocity interacting with the interface slope. In the eastern region, $h_x = O(\epsilon)$ while $h_y = O(\epsilon\beta)$. The zonal velocity in the eastern regime $u_2 = O(1)$ while the meridional velocity is stronger, $v_2 = O(\beta^{-1})$. The nonlinear advection term in the eastern regime, $\mathbf{v}_2 \cdot \nabla h$, is thus $O(\epsilon)$. Note that, because the flow is geostrophic, $\mathbf{v}_1 \cdot \nabla h = \mathbf{v}_2 \cdot \nabla h$.

In the western, topographically dominated, regime the dependence of the deep velocity on nonlinearity is calculated from the characteristic equations to be

$$u_2 = -\frac{w_i}{D_x}\left(1 - \frac{\epsilon\beta yP_y}{h}\right) + O(\epsilon^2). \qquad (21)$$

For upwelling mixing, $P_y < 0$, and increasing ϵ results in an increase in the strength of the deep zonal flow, as found in Fig. 4.

The zonal gradient of the interface in the western regime is calculated from (20) to be $O(\epsilon D_x P_y)$. The nonlinear term $u_2 h_x$ in the western regime is then $O(\epsilon P_y)$. The strength of the zonal flow P_y depends on the slope of the potential vorticity contours, as discussed earlier for the linear case. When the bottom slope is weak, so that the slope of the deep potential vorticity contour $yD_x/(D - h) \le O(1)$, the meridional pressure gradient scales as $P_y = O(\beta^{-1})$ and the nonlinear terms are then expected to be $O(\epsilon\beta^{-1})$. For steep bottom slopes of $D_x \ge O(\beta)$, the deep pressure gradient scales as $P_y = O(1)$ and the nonlinear terms are smaller, only $O(\epsilon)$. Thus, the nonlinear terms are expected to be most important in the western region when bottom slopes are weak but nonzero.

To understand how the nonlinear terms influence both the upper-layer and the deep-layer circulation, their effect on the vertical velocity needs to be considered. The vertical velocity may be expressed as the sum of the diapycnal velocity and the vertical component of the advection along the sloping interface that, for the western regime, is due to the zonal advection only. Conversely, one may think of the horizontal advection through the sloping interface as a component of the diapycnal advection. The result is the same for either interpretation:

$$w = w_i - u_2 h_x. \qquad (22)$$

For $w_i > 0$, the interface slopes upward toward the east and the deep velocity is eastward. The resulting nonlinear term is upward, in the same sense to the diapycnal velocity. If the diapycnal velocity is fixed (as is the case here), increasing the nonlinearity must also increase the vertical velocity by an amount $O(\epsilon P_y w_i)$.

Somewhat surprisingly, the nonlinear effect arising from the lateral advection along the sloping interface is
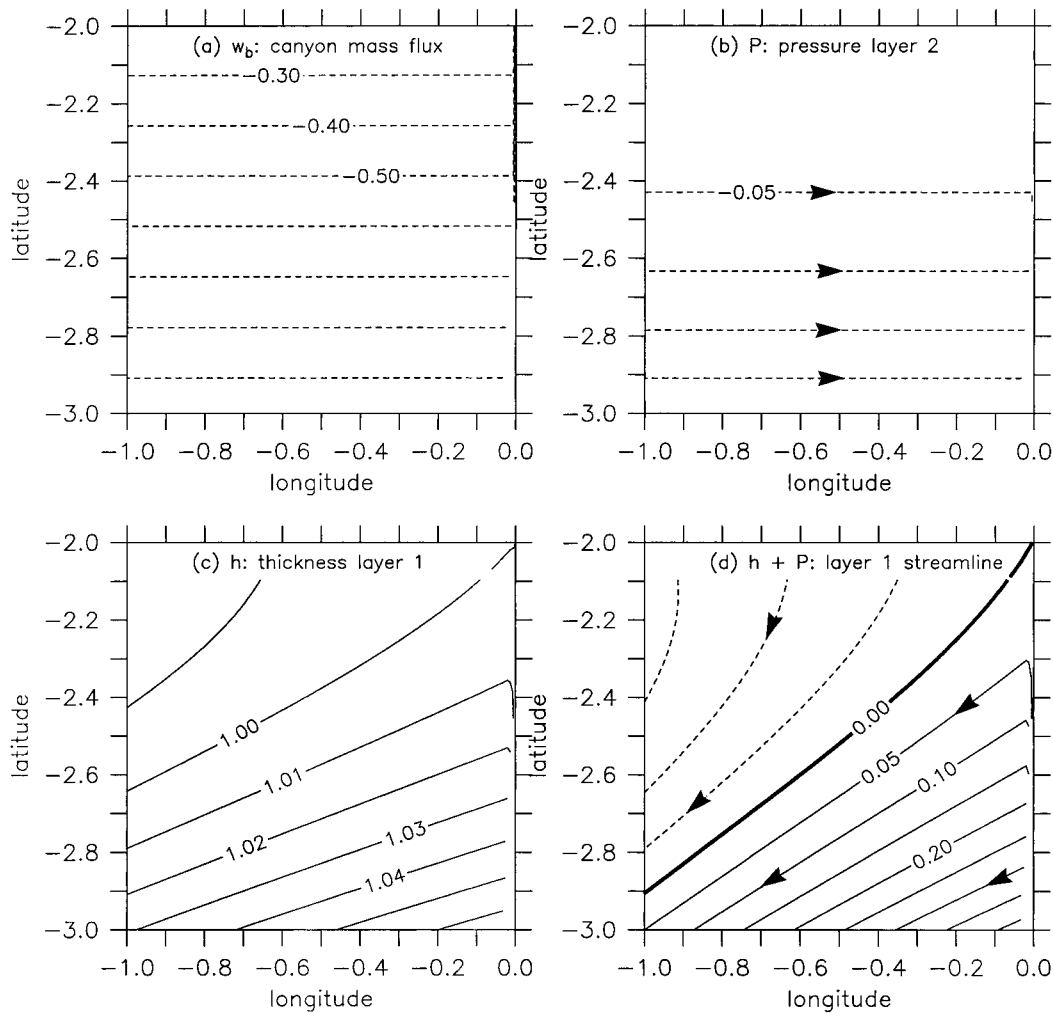
FIG. 7. Application to the abyssal Brazil Basin. (a) Distribution of downward mass flux into the deep canyons. (b) Pressure and flow direction in layer 2. (c) Thickness of layer 1. (d) Streamlines and flow direction in layer 1.

largest for weak bottom slopes. In this case, the change in the vertical velocity as a result of the nonlinear advection is $O(\epsilon\beta^{-1}w_i)$. The upper layer responds to this increase in the vertical velocity by an enhanced meridional flow, through the linear potential vorticity equation, that is of $O[\beta^{-1}(1 + \epsilon)]$, $\epsilon\beta^{-1}$ larger transport than for the linear case. Typical values for a midlatitude abyssal basin are $\beta \leq O(1)$ and $\epsilon \leq O(1)$.

When the bottom slope is large the nonlinear effects are greatly reduced. This is because the deep meridional pressure gradient $P_y = O(1)$ instead of the stronger recirculation of $O(\beta^{-1})$ found for weak bottom slopes. The enhancement of the upper-layer horizontal recirculation gyre is then $O(\beta^{-1} + \epsilon)$, a weaker dependence on nonlinearity than found for weak bottom slopes. These scaling results are consistent with the numerical calculations shown in Fig. 6a.

The effect of the nonlinear terms is reversed for a downwelling diapycnal velocity. In this case, the non-

linear term u_2h_x is still upward because both u_2 and h_x change sign. However, it is now in the opposite sense as the diapycnal velocity so that increasing ϵ reduces the vertical velocity at the interface and the upper-layer recirculation weakens, as found in Fig. 6b.

The stronger dependence of the nonlinear term on ϵ found for upwelling compared to downwelling arises because of the $O(\epsilon^2)$ terms neglected in Eq. (20). In physical terms, the enhanced upper-layer recirculation found for upwelling further increases the interface slope (through thermal wind), which then further increases the nonlinear terms. The reverse is found for a downward diapycnal mass flux; the interface slope relaxes slightly when the nonlinearities increase, acting to reduce further increases in the nonlinear effects.

Although the deep velocity in the western regime increases with increasing nonlinearity, Eq. (21), the flow remains zonal and the deep transport does not increase substantially. The flow remains zonal because the in-

west   east
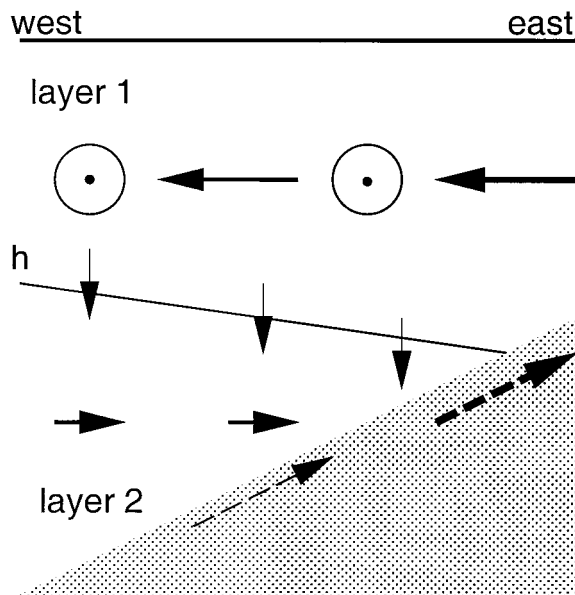
layer 1

h

layer 2

FIG. 8. Schematic of the circulation forced by diapycnal mixing over the western flank of the Mid-Atlantic Ridge in the abyssal Brazil Basin. The diapycnal mass flux is downward at the interface depth h and more strongly downward into the bottom canyons. The deep flow is weak and toward the east while the upper-layer flow is stronger and toward the southwest. The flow in the canyons is indicated schematically by the dashed arrows; it is not explicitly resolved in the model.

crease in w at the interface resulting from the nonlinear terms is exactly offset by an increase in the vertical velocity at the bottom, $u_2 D_x$. The stretching in the deep layer remains zero in the western regime. The deep transport does not increase substantially because the increase in deep velocity is largely offset by a decrease in the thickness of the deep layer (h increases toward the west).

4. Application to the Brazil Basin

The two-layer model is now configured to represent a region of mixing over the western flank of the Mid-Atlantic Ridge in the abyssal Brazil Basin. The measurements of Ledwell et al. (2000) and Polzin et al. (1997) indicate that the diapycnal mixing rate increases significantly toward the sloping bottom. A local heat balance indicates a downward mass flux that increases toward the bottom. As discussed by Ledwell et al. (2000) and St. Laurent et al. (2001), this is consistent with the downward spreading of a passive tracer released approximately 500 m over the tops of the deep canyons in the Mid-Atlantic Ridge. This tracer was found to spread into the canyons from above, and then to be carried eastward up the canyons toward the crest of the ridge. Deep in the canyons, the isopycnals become very steep and the eastward flowing water is mixed toward lighter density. This mixing scenario is repre-

sented in the two-layer model by a downward diapycnal flux at the interface h and a larger downward mass flux into the sloping bottom represented by w_b. The diapycnal upwelling that occurs deep in the canyons is not explicitly represented in the model. Its effect is included by introducing into layer 1, at the eastern edge of the mixing region where the interface intersects the topography, a mass flux equal to the total amount of water downwelled out of layer 2 into the canyons to the west. This is done through the specification of h at $x = 0$.

The model parameters are chosen as follows. The latitude of the model domain is centered at approximately 25° S, giving $f_0 = -5 \times 10^{-5}$ s^{-1} and $\beta* = 2 \times 10^{-11}$ m^{-1} s^{-1}. The thickness of the deep layer varies from 0 at the eastern limit of mixing to 1000 m toward the west over a distance of approximately 1000 km. The upper layer is taken to be 500 m thick over the crest of the ridge. Note that the model is applied only to the abyssal circulation, depths greater than approximately 3000 m. The spatial extent of the model domain is 10^6 m in both the zonal and meridional directions. The deep stratification $N^2 = 10^{-6}$ s^{-1}. The internal deformation radius $L_d = N\overline{H}/f_0 = 20 \times 10^3$ m, where $\overline{H}$ is a representative layer thickness taken to be 10^3 m.

The diapycnal velocity above the topography $w_i = -1 \times 10^{-7}$ m s^{-1} and is spatially uniform. Based on the inverse model results of St. Laurent et al. (2001), the mass flux into the canyons is specified to increase toward the pole as $w_b = w_{b0}[0.2 + 0.8(y - y_0)]$, where $w_{b0} = 1 \times 10^{-6}$ m s^{-1} and y_0 is the equatorward latitude of the mixing region. The downwelling into the canyons at the equatorward side of the region is approximately 6.3 m yr^{-1} and it increases linearly toward the pole to a maximum of 31.5 m yr^{-1}.

The nondimensional parameters of the model are now calculated. The vertical scale height $H = 500$ m, giving the upper-layer thickness on the eastern boundary $h_0 = 1$. The vertical velocity is scaled by $W = 10^{-6}$ m s^{-1} and the horizontal length scale $L = 10^6$ m so that the horizontal velocity scale $U = WL/H = 2 \times 10^{-3}$ m s^{-1}. The change in bottom depth of 10^3 m over 10^6 m zonal extent gives $D_x = -2.0$, resulting in the thickness of the deep layer vanishing at $x = 0$. The spatial scale of the mixing is relatively large compared to the central latitude of the region, so that $\beta = \beta*L/f_0 = 0.4$. The nonlinearity is significant with $\epsilon = U/\beta*L_d^2 = 0.25$.

The nondimensional mass flux into the deep canyons is shown in Fig. 7a, although the overall flow characteristics are not overly sensitive to the details of this meridional distribution. The deep pressure field is shown in Fig. 7b. As expected, the entire mixing region is in the western regime and the deep flow is zonal and toward the east. This deep flow is only sensitive to the difference between w_b and w_i. The eastward flow direction is required to supply the needed mass flux and is consistent with the stretching resulting from upwelling in the previous examples. The zonal flow increases

toward the south but is very weak throughout, with a basin average value $u_2 \approx 0.05$ cm s^{-1}.

The nondimensional depth of the interface h is shown in Fig. 7c. The interface shoals toward the west and toward the equator. The thickness of the upper layer varies by about 10%, or 50 m, over the 10^6 m extent of the model domain.

The flow in the upper layer is toward the southwest, along lines of constant $P + h$, as shown in Fig. 7d. There is a westward flow into the upper layer at $x = 0$, where the interface intersects the topography, forced by the return of the deep waters downwelled into the canyons. The direction of flow in the upper layer is generally southwest, with a maximum strength of approximately 0.25 cm s^{-1}. The direction of flow in the upper layer is sensitive to the difference between the middepth downwelling and the downwelling into the canyons. If the stretching of the deep layer is reduced, by either increasing w_i or decreasing w_b, the flow in the upper layer becomes more meridional. This is evident in Fig. 6d as w_b is decreased toward the equator. If the mixing at middepth is much less than the deep downwelling, as occurs toward the south, the upper-layer flow becomes more zonal. In the limit that the downwelling is all concentrated at the bottom, the upper-layer flow becomes purely zonal (not found here).

A schematic of the buoyancy-forced circulation in the deep and intermediate layers is shown in Fig. 8. The middepth diapycnal velocity is downward. There is also a downward mass flux into the deep canyons, represented here as a mass flux w_b through the bottom. The difference between the downward mass flux at middepth and the downward flux into the canyons is supplied by an eastward zonal flow in the deep layer. The deep flow remains zonal because the stretching provided by $w_i - w_b$ is exactly balanced by the interaction of the horizontal flow with the bottom $u_2 D_x$. This is true as long as $w_i - w_b$ is independent of x. This mass flux into the canyons is returned to the upper layer above where the deep layer intersects the topography, parameterizing the diapycnal upwelling that must take place within the canyons. The upper-layer flow is toward the west and toward the pole. The poleward flow is balanced dynamically by the middepth downwelling. This poleward sense of the flow is the same as found for the standard Stommel and Arons model, but the stretching is provided by w_i increasing toward the bottom, not by it increasing toward the main thermocline. The zonal flow recirculates some of the upwelled water into the mixing region, the remainder is advected out of the domain toward the southwest.

This general circulation pattern is similar to that calculated using an inverse model based on hydrographic and turbulence measurements by St. Laurent et al. (2001). Their circulation also produces a deep eastward flow into the canyons and a southwestward flow at middepths in the south and weaker southward flow in the northern part of the region. The strength of the deep eastward flow is $O(0.05$ cm s$^{-1})$, similar to that found here. The middepth flow is $O(0.3$ cm s$^{-1})$, only slightly stronger than that found in the present model.

The most fundamental difference between the present model and the inverse analysis is the sense of the horizontal component of the vertical velocity just above the ridge crests. St. Laurent et al. (2001) find that $\mathbf{v} \cdot \nabla h < 0$, indicating an upward contribution, while the present model finds $\mathbf{v} \cdot \nabla h > 0$. This arises because the deep flow is eastward and the interface deepens toward the east. Both of these characteristics are also found in the inverse model, but the eastward flow is confined much more closely toward the bottom. The discrepency may be an artifact of the limited vertical resolution of the two-layer model, or the manner in which the mass flux into the canyons is treated. In any case, the nonlinear contribution is only $O[\epsilon w_i(w_b - w_i)] = 0.05$. If the middepth mixing $w_i = 0$, the upper-layer flow is zonal so $h_x = 0$ (so that $\mathbf{v} \cdot \nabla h = 0$), while if $w_b = w_i$, then the nonlinear term vanishes because $u_2 = 0$.

While some similarities with the data are expected because the model forcing was drawn from the analysis of St. Laurent et al. (2001), there are several important aspects of the circulation that are not imposed. The strength of the deep flow is very weak in spite of the strong turbulent mixing. This is because the bottom pressure torque term balances the vertical stretching, as discussed in the previous idealized problems. This importance of the topographic interaction is inevitable for such strong topography and is not a consequence of details in the model forcing. The direction of the deep- and upper-layer flows are also not specified and, if one neglects this topographic interaction, there would be a strong meridional component to the deep flow, in disagreement with the inverse model results of St. Laurent et al. (2001). This barotropic component of the flow also alters the direction of the flow in the upper layer. The simple examples in section 3 clearly demonstrate the dynamics in this topographically dominated regime. This application to the Brazil Basin suggests that similar dynamics are important there.

5. Summary

The large-scale circulation forced by diapycnal mixing over a sloping bottom is considered. A simple nonlinear, two-layer planetary geostrophic model is developed in which the circulation is forced by diapycnal mixing between the fluid layers and by a downward mass flux into deep (unresolved) canyons in the sloping bottom. Analytic linear and nonlinear solutions and direct numerical integration of the characteristic equations are provided. Novel aspects of this study include the influences of nonlinearities in the density equation on the abyssal and upper ocean flow, the circulation required to balance *localized* mixing regions over a sloping bottom, and the dependence of the deep and inter-

mediate circulations on a mixing rate that increases toward a sloping bottom.

For a flat bottom, the familiar beta-plume horizontal recirculation is reproduced. However, when topography is introduced such that the topographic Rossby wave phase speed exceeds the baroclinic planetary Rossby wave phase speed, the strong beta-plume recirculation is replaced by a weak zonal flow in the deep layer. The mass budget and vorticity balances in this topographically dominated regime are entirely different than are found in the beta-plume regime, which becomes confined ever more closely to the eastern boundary.

Nonlinearities, as measured by the ratio of the advective speed to the Rossby wave phase speed, can either enhance or reduce the strength of the upper-layer recirculation and are shown to be most important for weak, but nonzero, bottom slopes. Nonlinearity also forces the characteristics, or geostrophic contours, to cross isolines of potential vorticity when bottom topography is present. This can result in regions of closed potential vorticity contours that are not isolated dynamically from the rest of the abyss but instead directly forced by turbulent mixing over the sloping bottom.

The model is applied to the region of strong diapycnal mixing over the western flank of the Mid-Atlantic Ridge in the abyssal Brazil Basin. The model is forced by a downward mass flux at the interface above the topography and a stronger downward mass flux into the deep canyons of the ridge. This flow into the canyons is returned to the upper layer where the deep layer intersects the bottom. The model produces a weak eastward flow in the deep layer and a stronger southwestward flow in the upper layer. This general strength and circulation pattern are in reasonable agreement with recent observations and inverse model results in the Brazil Basin (Ledwell et al. 2000; St. Laurent et al. 2001). It is found here that bottom pressure torque is essential to producing such a sluggish deep flow in the presence of very strong turbulent mixing.

These results identify the basic nondimensional parameters that control the large-scale deep circulation forced by diapycnal mixing over a sloping bottom. The primary influence of the sloping bottom is to introduce a new flow regime in which the deep flow is zonal. Although details of the mass balance differ, this zonal flow regime persists even when nonlinearities in the density equation become large. Bottom slopes that are typical of the abyssal ocean are sufficiently steep that most of the deep ocean is expected to be in this topographically dominated regime. In addition, the vertical velocity does not need to be exactly balanced by the diapycnal mass flux, as is often assumed in simple models of the abyssal circulation, and significant differences can be expected as the advective speed approaches the Rossby wave phase speed.

APPENDIX

The Characteristic Equations

The characteristic equations are derived for the two-layer planetary geostrophic fluid over a sloping bottom. Similar derivations can be found, for example, in Luyten and Stommel (1986) and Hautala and Riser (1989). Although similar in approach, the formulation here differs from each of these previous models in important ways.

The velocities in the deep layer u_2 and v_2 are related to variations in the deep dynamic pressure P through the geostrophic relations as

$$u_2 = -\frac{g'P_y}{f}, \qquad v_2 = \frac{g'P_x}{f}, \qquad \text{(A1)}$$

where the subscripts (x, y) indicate the partial derivative (note that P has dimensions of length). The Coriolis parameter is assumed to vary linearly with latitude as $f = f_0 + \beta^* y$. The velocities in the upper layer are calculated relative to the deep velocities using the thermal wind relation as

$$u_1 = -\frac{g'(P + h)_y}{f}, \qquad v_1 = \frac{g'(P + h)_x}{f}. \quad \text{(A2)}$$

The continuity equation for the upper layer is written as

$$(hu_1)_x + (hv_1)_y = w_i, \qquad \text{(A3)}$$

while the continuity equation for layer 2 is

$$[(D - h)u_2]_x + [(D - h)v_2]_y = w_b - w_i. \quad \text{(A4)}$$

The main difference between the present model and that of Luyten and Stommel (1986) is the introduction of a finite bottom depth. This introduces some additional terms, and results in a nonlinear system of equations, but allows for the consideration of stretching at the bottom and the resulting barotropic motion. The equations retain the nonlinear advection terms in the density equation ($\mathbf{v} \cdot \nabla h$) and also permit the thickness of the deepest layer to vanish by intersecting tall topography. The application in mind is the large-scale circulation forced by mixing over topography in the ocean abyss, so that, for simplicity, wind forcing at the surface has been neglected.

The barotropic vorticity equation is derived by substituting the geostrophic relations into the continuity equations and adding:

$$\frac{\beta}{f}(hh_x + DP_x) = -\frac{f}{g'}w_b - D_xP_y. \qquad (A5)$$

This result is similar to that obtained by LS and HR, the main difference being the additional term on the right-hand side that results from the interaction of the zonal flow in layer 2 with the sloping bottom (D_xP_y). This gives rise to a vertical velocity at the bottom and can thus drive a barotropic flow. This term is the equivalent of the generalized bottom pressure torque term discussed by Holland (1973) and Mertz and Wright (1992). Note that the mixing rate w_i does not appear explicitly in (A5); however, it is shown that the barotropic flow is not independent of w_i because of the bottom interaction term D_xP_y.

Hautala and Riser included wind forcing and bottom topography in a similar three-layer model, but the influences of the bottom topography on the upper and middepth ocean were neglected. This allowed them to solve for the upper-ocean circulation and layer depths independent of the bottom topography and bottom pressure torque terms. It will be shown that the interaction of the abyssal flow with the bottom does alter the upper-layer circulation, most strongly for weak, but nonzero, bottom slopes.

An expression for the thickness of the upper layer may be found by integrating (A5) in the zonal direction from the eastern boundary:

$$h^2 = h_0^2 - 2(S_1 + S_2 + W_B). \qquad (A6)$$

The thickness of the upper layer on the eastern boundary is h_0, which may be a function of y. The right-hand side terms are defined as

$$S_1 = \int_0^x \frac{fD_xP_y}{\beta}\, dx, \qquad S_2 = \int_0^x DP_x\, dx,$$

$$W_B = \int_0^x \frac{f^2w_b}{g'\beta}\, dx. \qquad (A7)$$

The first term S_1 represents the integrated upwelling at the bottom resulting from the interaction between the zonal flow and the sloping bottom. The second term S_2 is proportional to the integrated meridional transport in the deep layer. The third term is the integrated mass flux into the bottom topography (canyons). Equation (A6) represents the linear vorticity balance. The difference between the net vertical motion at the bottom (first and third terms) and the meridional transport represented by the zonal gradient in the deep pressure gives rise to a zonal slope in the interface between layers 1 and 2 and meridional flow in layer 1 such that the barotropic linear vorticity balance is satisfied. The terms S_1 and S_2 depend on the strength of the deep flow.

Following LS, the zonal and meridional gradients of h may be calculated from (A6) and substituted back into the layer 2 continuity equation (A4). The result may be written as

$$\left[(S_1 + W_B + S_3)_y - \frac{\beta h(D - h)}{f}\right]P_x$$

$$+ \left[-hD_x - \frac{fD_xP_y}{\beta} - \frac{f^2w_b}{g'\beta}\right]P_y$$

$$= \frac{fh}{g'}(w_b - w_i), \qquad (A8)$$

where

$$S_3 = \int_0^x D_xP\, dx. \qquad (A9)$$

Luyten and Stommel and HR derive similar equations that are linear in P, which they solved using the method of characteristics. The characteristic slopes are given by the coefficients of the P_x and P_y terms and the change in P along the characteristic path is given by the right-hand side. The addition of bottom topography introduces the nonlinear terms S_1, S_3, and the term proportional to P_y^2. Nonetheless, the equations may be solved by following a similar approach and iterating to include the nonlinear terms, as outlined in section 2.

Although it is instructive to carry out the derivation using dimensional variables, the dependence of the solutions on the model parameters is made clear by considering nondimensional forms of the equations. The following scaling is appropriate for a nearly geostrophic flow with similar dominant spatial scales in the zonal and meridional directions and interface displacements and bottom depth changes that are as large as the mean layer thicknesses:

$$u, v \propto U, \qquad P \propto \frac{UfL}{g'}, \qquad h, D \propto H,$$

$$x, y \propto L, \qquad f \propto \frac{f_0y}{y_0}, \qquad w_b, w_i \propto \frac{UH}{L}.$$

The equations presented in section 2 result from substituting this scaling into Eqs. (A6), (A7), (A8), and (A9). All equations solved in the body of the paper use nondimensional variables. The characteristics are interpreted, and the solution procedure is outlined, in section 2.

REFERENCES

Hautala, S. L., and S. C. Riser, 1989: A simple model of abyssal circulation, including effects of wind, buoyancy, and topography. *J. Phys. Oceanogr.,* **19,** 596–611.

Holland, W. R., 1973: Baroclinic and topographic influences on the transport in western boundary currents. *Geophys. Fluid Dyn.,* **4,** 187–210.

Joyce, T. M., and K. G. Speer, 1987: Modeling the large-scale influence of geothermal sources on abyssal flow. *J. Geophys. Res.,* **92,** 2843–2850.

Kawase, M., 1993: Effects of a concave bottom geometry on the upwelling-driven circulation in an abyssal basin. *J. Phys. Oceanogr.,* **23,** 400–405.

——, and D. Straub, 1991: Spinup of source-driven circulation in an

abyssal basin in the presence of bottom topography. *J. Phys. Oceanogr.,* **21,** 1501–1514.

Ledwell, J. R., E. T. Montgomery, K. L. Polzin, L. C. St. Laurent, R. W. Schmitt, and J. M. Toole, 2000: Mixing over rough topography in the Brazil Basin. *Nature,* **403,** 179–182.

Luyten, J., and H. Stommel, 1986: Gyres driven by combined wind and buoyancy flux. *J. Phys. Oceanogr.,* **16,** 1551–1560.

Mertz, G., and D. G. Wright, 1992: Interpretations of the JEBAR term. *J. Phys. Oceanogr.,* **22,** 301–305.

Pedlosky, J., 1987: *Geophysical Fluid Dynamics.* Springer-Verlag, 710 pp.

——, 1992: The baroclinic structure of the abyssal circulation. *J. Phys. Oceanogr.,* **22,** 652–659.

——, 1996: *Ocean Circulation Theory.* Springer-Verlag, 453 pp.

Polzin, K. L., J. M. Toole, J. R. Ledwell, and R. W. Schmitt, 1997: Spatial variability of turbulent mixing in the abyssal ocean. *Science,* **276,** 93–96.

Spall, M. A., 2000: Buoyancy-forced circulations around islands and ridges. *J. Mar. Res.,* **58,** 957–982.

St. Laurent, L. C., J. M. Toole, and R. W. Schmitt, 2001: Buoyancy forcing by turbulence above rough topography in the abyssal Brazil Basin. *J. Phys. Oceanogr.,* in press.

Stommel, H. M., 1982: Is the South Pacific helium-3 plume dynamically active? *Earth Planet. Sci. Lett.,* **61,** 63–67.

——, and A. B. Arons, 1960: On the abyssal circulation of the world ocean—II. An idealized model of the circulation pattern and amplitude in oceanic basins. *Deep-Sea Res.,* **6,** 217–233.

Straub, D., and P. B. Rhines, 1990: Effects of large-scale topography on abyssal circulation. *J. Mar. Res.,* **48,** 223–253.

——, P. D. Killworth, and M. Kawase, 1993: A simple model of mass-driven abyssal circulation over a general bottom topography. *J. Phys. Oceanogr.,* **23,** 1454–1469.